Symmetry classification of uniform states in spin-2 Bose-Einstein condensates and neutron $^3P_2$ superfluids

Michikazu Kobayashi

School of Environmental Science and Engineering, Kochi University of Technology, Miyanoguchi 185,
Tosayamada, Kami, Kochi 782-8502, Japan

Muneto Nitta

Department of Physics, and Research and Education Center for Natural Sciences, Keio University, Hiyoshi 4-1-1,
Yokohama, Kanagawa 223-8521, Japan

We clarify a relation between the Gross-Pitaevskii energy functional for spin-2 spinor Bose-Einstein condensates and the Ginzburg-Landau theory for neutron $^3P_2$ superfluidis (spin-triplet P-wave pairing with total angular momentum two). We then classify all uniform states with nontrivial unbroken symmetries with the help of geometric invariant theory.

I. INTRODUCTION

Condensations can have spin and angular momentum degrees of freedom. Superfluids ^{3}He having both spin-triplet ($S = 1$) and P-wave ($L = 1$) parings are such an example confirmed in nature [1,2]. Among such condensations total-spin two ($J = 2$) condensates consist of $2J + 1 = 5$ complex degrees of freedom, and the Ginzburg-Landau (GL) theory for $J = 2$ condensates was first studied by Mermin [3] in which possible ground states were classified. Nematic, cyclic, and ferromagnetic phases are typical phases. In nature, at least two examples of such condensations are known. One is spin-2 ($S = 2$) spinor Bose-Einstein condensations (BECs), which were realized in laboratory experiments. The other is $^3P_2$ neutron superfluids consisting of neutron Cooper pairs of spin-triplet and P-wave paring with the total angular momentum $J = 2$, relevant for neutron star cores.

Spin-2 spinor BECs can be theoretically well described by the Gross-Pitaevskii (GP) equations and GP energy functional; see Ref. [4] as a review. There are typically three phases, cyclic, nematic, and ferromagnetic phases, and many interesting physics can be expected in each phase. Experimentally, spin-2 BECs are realized by ^{87}Rb atoms, and the phase is around the boundary between cyclic phase and ferromagnetic phase [5–10].

In the cyclic phase, the order parameter manifold (OPM) parametrized by Nambu-Goldstone (NG) modes associated with spontaneous symmetry breaking is $[U(1) \times SO(3)]/T$ with a tetrahedral group T [11]. Due to the nontrivial first homotopy group $\pi_1 \simeq \mathbb{Z} \times_h T^*$ ($\times_h$ is a product defined in Ref. [12], and T^* is the universal covering group of T), 1/3 quantized non-Abelian vortices are allowed [13–15]. Two vortices belonging to noncommutative elements of π_1 do not reconnect in collisions, instead creating a rung vortex

connecting them [14]. 3D skyrmions based on the third homotopy group π_3 are allowed in the cyclic phase [16].

The nematic phase consists of three subphases continuously degenerated with each other: uniaxial nematic (UN), D_2 biaxial nematic (D_2BN), and D_4 biaxial nematic (D_4BN) phases, where D_n is a dihedral group of order n. The OPMs are $U(1) \times SO(3)/O(2) \simeq S^1 \times \mathbb{R}P^2$, $U(1) \times SO(3)/D_2$, and $[U(1) \times SO(3)]/D_4$ of dimensions three, four, and four, respectively. These are connected by a parameter of continuous degeneracy [17], which can be regarded as a quasi-NG mode associated with symmetry breaking of an enhanced symmetry [18], and these OPMs are submanifolds of an extended OPM $[S^1 \times S^4]/\mathbb{Z}_2$ parametrized by both the NG and quasi-NG modes. This continuous degeneracy can be lifted by quantum corrections [17,18]. In the nematic phase, 1/2 quantized non-Abelian vortices are allowed [19]. As in the cyclic phase, 3D skyrmions are also allowed in the BN phase [16].

On the other hand, the neutron $^3P_2$ superfluids are relevant in the core of neutron stars [20–39]. See Refs. [35,39–43] as a review from more general perspectives of superfluidity and superconductivity in neutron stars, including neutron $^3P_2$ superfluids. The existence of $^3P_2$ superfluids was indicated from astrophysical observations of the rapid cooling of a neutron star in Cassiopeia A [44–46]. The GL theory as a bosonic effective theory around the transition point from the normal phase to the superfluid was established previously [25,26,47–55]. The ground state in the weak-coupling limit was determined to be the nematic phase [47]. In the GL free energy up to the fourth order, there is a continuous degeneracy among UN, D_2BN, and D_4BN phases as the case of spin-2 BECs while a coupling to the magnetic field lifts the degeneracy, picking up the D_4BN state as the ground state [47]. In the absence of a magnetic field, the next-leading order of the GL expansion, namely, the sixth order, lifts the degeneracy picking the UN phase as a possible ground state [47]. In the

presence of the magnetic field, either UN, D_2BN, or D_4BN states can be the ground states depending on the strength of the magnetic field [51]. However, at this order, the ground states are not global minima but just local minima because of the instability caused by the sixth-order terms at large values of the condensates. Thus, the GL free energy expanded up to the eighth order is needed to determine the unique ground states [54]. In the GL theory, bosonic excitations as collective modes in the $^3P_2$ superfluids were discussed [56–68], which are relevant for cooling process of neutron stars. Several kinds of vortices were discussed within the GL theory, such as integer vortices [25,48,49,51,69], half-quantized non-Abelian vortices [70], and coreless vortices [71]. Other topological defects such as domain walls [72] and topological defects on the boundary (called boojums) of $^3P_2$ superfluids [73] were also found.

The Bogoliubov-de Gennes (BdG) equation offers a framework beyond the GL theory to deal with fermion degrees of freedom. The phase diagram in the plane of the temperature and magnetic field was determined in the BdG equation [74]. A tricritical point connecting first- and second-order phase transitions between D_4 and D_2 BN phases was found [74,75]. A topological superfluidity was also found [74], yielding topologically protected Majorana zero modes on the boundary of $^3P_2$ superfluids [74] and an integer vortex core [76] as well as half-quantized vortex core [77].

Thus far, the so-called quasiclassical approximation linearizing dispersions around the Fermi surface was used to obtain nematic ground states in both the GL theory and BdG equation. Without the quasiclassical approximation, novel ground states were found around the critical temperature in the presence of strong magnetic fields: a ferromagnetic state and magnetized BN states (also called broken axisymmetric states in spin-2 BECs [4]) interpolating the ferromagnetic state and nematic state [78].

On the other hand, spin-2 BECs are closely related as one of candidates by astrophysical laboratories for neutron stars [42,43]. The low-energy theories such as GP theory for spinor BECs and GL theory for neutron superfluids give an important viewpoint to connect these systems. However, these two theories have been explored independently: condensates of spin-2 BECs are usually described by five component condensates ψ and a 3×3 traceless symmetric tensor A are used for $^3P_2$ superfluids in the literature, thus looking different at first glance. However, since they are both $J = 2$ condensates, they can be mapped to each other. The GP and GL energy functionals are quite similar after rewriting them, consequently admitting similar objects such as half-quantized non-Abelian vortices, [19] and [70], respectively. Nevertheless they are not exactly the same. Apparent differences are, for instance, the following: (1) the GP theory contains up to the fourth order of the condensates, while the GL theory is basically expansion of the condensates, thus containing infinitely higher orders; (2) gradient terms are different: two tensor indices of the condensates of the spin-2 spinor BECs are both spins which are internal degrees of freedom, while one of two indices of the condensates of $^3P_2$ superfluids represents the angular momentum, which can be contracted with spatial derivatives, thus admitting more gradient terms; and (3) a magnetic field interacts with the condensates in different ways. These differ-

ences bring differences beyond topology such as stability and dynamics.

The purpose of this paper is to clarify a relation between spin-2 spinor BECs and $^3P_2$ superfluids. To this end, it turns out to be useful to use the geometric invariant theory (see, e.g., Refs. [79–81]); since there are five condensations, the configuration space is $\mathbb{C}^5$. The symmetry of the system is $U(1) \times SO(3)$, and then inequivalent configurations can be expressed by the "moduli space of vacua" $\mathbb{C}^5/[U(1) \times SO(3)]$, parametrized by six $U(1) \times SO(3)$ invariants. The symmetry classification of spin-2 spinor BECs have been investigated in terms of three invariants (among the totally six invariants) manifestly appearing in the low-energy Hamiltonian [4,17,18,82–86]. Here we introduce remaining three invariants absent in the low-energy Hamiltonian of spin-2 BECs. With a help of all these six invariants, we rewrite the energy functional of spin-2 BECs in terms of a traceless symmetric tensor, and that of $^3P_2$ superfluids in terms of five component condensates. We find that in order to rewrite the latter in terms of the invariants, all six invariants are needed. We further classify all possible uniform states with nontrivial unbroken symmetries as candidates of ground states or metastable states and clarify how they are connected in the moduli space.

This paper is organized as follows. In Sec. II we introduce the standard formulations of spin-2 BECs and $^3P_2$ superfluids. In Sec. III we specify a relation between them, and in Sec. IV uniform states with nontrivial unbroken symmetries are classified as candidates of the ground states or metastable states. Section V describes $^3P_2$ superfluids, and Sec. VI is devoted to a summary and discussion.

II. FORMULATION

In this section, we introduce the standard formulations of the GP energy functional of spin-2 BECs in terms of five component condensates, and the GL theory for $^3P_2$ superfluids in terms of a 3×3 traceless symmetric tensor.

A. Spin-2 spinor Bose-Einstein condensates

The effective low-energy Hamiltonian density h of spin-2 spinor BECs can be written as

$$h = h_0 + h_{qz} + h_{int},$$

$$h_0 = \frac{\hbar^2}{2m_b} \boldsymbol{j}^\dagger \boldsymbol{j},$$

$$h_{qz} = q \sum_{i,j=x,y,z} B_i (\psi^\dagger \hat{S}_i \hat{S}_j \psi) B_j, \quad (1)$$

$$h_{int} = \sum_{S=0}^{4} \frac{g_S}{2} \sum_{M=-S}^{S} \sum_{m_1,\dots,m_4=-2}^{2} C_{2m_1,2m_2}^{SM} C_{2m_3,2m_4}^{SM}$$
$$\times \psi_{m_1}^* \psi_{m_2}^* \psi_{m_3} \psi_{m_4},$$

where $\psi = (\psi_2 \quad \psi_1 \quad \psi_0 \quad \psi_{-1} \quad \psi_{-2})^T$ is the five-component condensate order parameters of a spin-2 BEC, $\boldsymbol{j} = -i\boldsymbol{\nabla}\psi$ is the current density, m_b is the mass of bosons, and $\hat{S}_i$ ($i = x, y, z$) are 5×5 spin-2 matrices. In the quadratic Zeeman energy part h_{qz}, $q = (g\mu_B)^2/E_{hf}$ is the coefficient of the

quadratic Zeeman energy under the magnetic field $\boldsymbol{B}$ with the Landé g-factor g, the Bohr magneton μ_B, and the hyperfine energy splitting E_{hf}. In the interaction part h_{int}, g_S is the coupling constant in the total spin S channel, and $C^{SM}_{s_1 m_1, s_2 m_2}$ are the Clebsch-Gordan coefficients.

The interaction part of the Hamiltonian density h_{int} can be rewritten as

$$h_{\mathrm{int}} = \frac{1}{2}\big(c_0 \rho^2 + c_1 \boldsymbol{S}^2 + c_2 |\Psi_{20}|^2\big),$$
$$\rho = \psi^\dagger \psi, \quad \boldsymbol{S} = \psi^\dagger \hat{\boldsymbol{S}} \psi, \tag{2}$$
$$\Psi_{20} = \psi^T \hat{T} \psi = \sqrt{5} \sum_{m_1, m_2 = -2}^{2} C^{00}_{2m_1, 2m_2} \psi_{m_1} \psi_{m_2},$$

where the coupling constants are defined by $c_0 = (4g_2 + 3g_4)/7$, $c_1 = (g_4 - g_2)/7$, $c_2 = (7g_0 - 10g_2 + 3g_4)/35$. ρ, $\boldsymbol{S}$, and Ψ_{20} are known as the density, the spin density, and the singlet-pair amplitude with the time reversal operator $\hat{T}$ defined as $(\hat{T}\psi)_m = (-1)^m \psi_{-m} \equiv \varphi_m$. Note that ρ^2, $\boldsymbol{S}^2$, and $|\Psi_{20}|^2$ are typical U(1) × SO(3) invariants.

In the absence (presence) of the magnetic field $B = 0$ ($B \neq 0$), the energy density is invariant under the transformation $\mathcal{G}_{\mathrm{b}}(\varphi, \boldsymbol{n}, \theta)\psi = e^{i\varphi} e^{-i\hat{S}\cdot\boldsymbol{n}\theta}\psi$ ($\mathcal{G}_{\mathrm{b}}(\varphi, \boldsymbol{B}/|\boldsymbol{B}|, \theta)\psi = e^{i\varphi} e^{-i\hat{S}\cdot(\boldsymbol{B}/|\boldsymbol{B}|)\theta}\psi$), giving the symmetry $G_{\mathrm{b}} = $ U(1) × SO(3) [$G_{\mathrm{b}} = $ U(1) × SO(2)] of the energy density.

B. Ginzburg-Landau free energy for $^3P_2$ neutron superfluids

Here we briefly review the GL theory for $^3P_2$ superfluids in terms of a traceless symmetric tensor. The original partition function of nonrelativistic two-spinor field $\varphi(t, \boldsymbol{x}) =$ $(\varphi_\uparrow \ \ \varphi_\downarrow)^T$ for a neutron is

$$Z = \int \mathcal{D}\varphi \, \mathcal{D}\varphi^* \mathcal{D}A \, \mathcal{D}A^* \exp\left(-\int d\tau \, d\boldsymbol{x} \, \mathcal{L}\right), \tag{3}$$

where $\tau \in [0, 1/T]$ is the imaginary time it with the temperature T. $\mathcal{L}$ is the Lagrangian density with the imaginary time τ as

$$\mathcal{L} = \mathcal{L}_0 + \mathcal{L}_{\mathrm{int}},$$
$$\mathcal{L}_0 = \varphi^*\left(\partial_\tau + \frac{\nabla^2}{2m_{\mathrm{n}}} + \mu + \boldsymbol{\mu}_{\mathrm{n}} \cdot \boldsymbol{B}\right)\varphi, \tag{4}$$
$$\mathcal{L}_{\mathrm{int}} = \sum_{i,j=x,y,z}\left(A^{*ab}T^{ab} + T^{*ab}A^{ab} + \frac{A^{*ab}A^{ab}}{G}\right),$$

where $\boldsymbol{B}$ is the external magnetic field, and $\boldsymbol{\mu}_{\mathrm{n}} = -\hbar\gamma_{\mathrm{n}}\boldsymbol{\sigma}/2$ is the magnetic momentum with the Pauli matrices $\boldsymbol{\sigma}$ and the neutron gyromagnetic ratio γ_{n} in the noninteracting Lagrangian density $\mathcal{L}_0$. In the interacting Lagrangian density $\mathcal{L}_{\mathrm{int}}$, G is the renormalized coupling constant, T^{ab} is the tensor operator for the repulsive interaction, and A^{ab} is the auxiliary tensor field having symmetric and traceless form.

Near the transition temperature T_{c} for neutron $^3P_2$ superfluidity, the original partition function (3) gives the GL free-energy density f as [54]

$$f = K_0\big(f_{202}^{(0)} + f_{202}^{(1)}\big) + \alpha f_{002} + \beta_0 f_{004} + \gamma_0 f_{006}$$
$$+ \delta_0 f_{008} + \beta_2 f_{022} + \gamma_2 f_{024}$$
$$+ \sum_{4l+2m+n=10} O(\partial^l |\boldsymbol{B}|^m \mathrm{A}^n). \tag{5}$$

Each term in the free-energy density f can be written as

$$f_{202}^{(0)} = \sum_{i,j,k=x,y,z} \partial_i A_{jk} \partial_i A_{jk}^*, \quad f_{202}^{(1)} = \sum_{i,j,k=x,y,z}(\partial_i A_{ji}\partial_k A_{jk}^* + \partial_i A_{jk}\partial_k A_{ji}^*),$$

$$f_{002} = (\mathrm{tr}A^*A), \quad f_{004} = (\mathrm{tr}A^*A)^2 - (\mathrm{tr}A^{*2}A^2),$$

$$f_{006} = -24(\mathrm{tr}A^*A)^3 + 36(\mathrm{tr}A^*A)(\mathrm{tr}A^{*2}A^2) - 6|\mathrm{tr}A^*A^2|^2 + \frac{10}{3}|\mathrm{tr}A^3|^2,$$

$$f_{008} = 192(\mathrm{tr}A^*A)^4 - 384(\mathrm{tr}A^*A)^2(\mathrm{tr}A^{*2}A^2) - 64(\mathrm{tr}A^*A)|\mathrm{tr}A^3|^2 + 144(\mathrm{tr}A^{*2}A^2)^2 + 192(\mathrm{tr}A^*A)|\mathrm{tr}A^*A^2|^2 \tag{6}$$
$$- 48|\mathrm{tr}A^*A^2|^2(\mathrm{tr}A^{*2}A^2) + 12|\mathrm{tr}A^*A^2|^4 - 96\,\mathrm{Re}[(\mathrm{tr}A^2)(\mathrm{tr}A^{*2}A)^2],$$

$$f_{022} = \boldsymbol{B}^T(A^*A)\boldsymbol{B},$$

$$f_{024} = \boldsymbol{B}^2[-2(\mathrm{tr}A^{*2})(\mathrm{tr}A^2) - 4(\mathrm{tr}A^*A)^2 + 4(\mathrm{tr}A^*AA^*A) + 8(\mathrm{tr}A^{*2}A^2)]$$
$$+ 2\,\mathrm{Re}[(\mathrm{tr}A^2)(\boldsymbol{B}^T A^{*2}\boldsymbol{B})] - 8(\mathrm{tr}A^*A)(\boldsymbol{B}^T A^*A\boldsymbol{B}) + 4\boldsymbol{B}^T[\mathrm{Re}(A^*A^2A^*) - 2A^*AA^*A - 2A^{*2}A^2]\boldsymbol{B}.$$

The GL coefficients can be calculated in the weak coupling limit within the quasiclassical approximation as [54]

$$K_0 = \frac{7\zeta(3)N(0)p_{\mathrm{F}}^4}{240\pi^2 m_{\mathrm{n}}^2 T^2}, \quad \alpha = \frac{N(0)p_{\mathrm{F}}^2}{3}\log\frac{T}{T_{\mathrm{c}}},$$

$$\beta_0 = \frac{7\zeta(3)N(0)p_{\mathrm{F}}^4}{60\pi^2 T^2}, \quad \gamma_0 = \frac{31\zeta(5)N(0)p_{\mathrm{F}}^6}{13\,440\pi^4 T^4},$$

$$\delta_0 = \frac{127\zeta(7)N(0)p_{\mathrm{F}}^8}{387\,072\pi^6 T^6}, \quad \beta_2 = \frac{7\zeta(3)N(0)p_{\mathrm{F}}^2\gamma_{\mathrm{n}}^2}{48(1+F_0^a)^2\pi^2 T^2},$$

$$\gamma_2 = \frac{31\zeta(5)N(0)p_{\mathrm{F}}^4\gamma_{\mathrm{n}}^2}{3840(1+F_0^a)^2\pi^4 T^4}, \tag{7}$$

with the neutron mass m_{n}, the Fermi momentum p_{F}, the state-number density $N(0) = m_{\mathrm{n}}p_{\mathrm{F}}/(2\pi)^2$ at the Fermi surface,

and the Landau parameter F_0^a defined as the modification of the magnetic momentum $|\boldsymbol{\mu}| = (\gamma_n \hbar/2)/(1 + F_0^a)$. The GL free energy without the quasiclassical approximation was also calculated in Ref. [78].

One can consider the transformation with the spin-orbit locked symmetry

$$\bar{\mathcal{G}}_n(\varphi, \boldsymbol{n}, \theta)A = e^{i\varphi}R(\boldsymbol{n}, \theta)AR(\boldsymbol{n}, \theta)^T, \tag{8}$$

where $e^{i\varphi}$ denotes the global $U(1)$ phase shift and $R(\boldsymbol{n}, \theta)$ denotes spin-orbit locked rotation with the rotation axes $\boldsymbol{n}$ and rotation angles θ. The free-energy density is invariant under the transformation shown in Eq. (8) in the absence of the magnetic field $\boldsymbol{B} = 0$, showing the symmetry $G_n \simeq U(1) \times SO(3)$ for the free energy.

In the presence of the magnetic field $\boldsymbol{B} \neq 0$, the symmetry G_n is explicitly broken by the background to $G_n \simeq U(1) \times SO(2)$, where the rotational axis $\boldsymbol{n}$ is fix to be parallel to $\boldsymbol{B}$.

III. RELATION BETWEEN NEUTRON SUPERFLUIDITY AND SPIN-2 SPINOR CONDENSATES

In this section, we rewrite the free-energy density f for neutron $^3P_2$ superfluids and the energy density h for spin-2 spinor condensates in terms of the condensate order parameter ψ and the tensor field A, respectively, by introducing a map between them.

A. Spin-2 spinor BECs in terms of a traceless symmetric tensor A

We begin with considering the spherical harmonic form Y_ψ for the condensate wave function ψ in Eq. (2) as

$$Y_\psi = \sum_{m=-2}^{2} Y_{2m}(\boldsymbol{n})\psi_m, \tag{9}$$

where $Y_{2m}(\boldsymbol{n})$ is the rank-2 spherical harmonic functions

$$Y_{2\pm2} = \frac{1}{4}\sqrt{\frac{15}{2\pi}}(n_x \pm in_y)^2,$$

$$Y_{2\pm1} = \mp\frac{1}{2}\sqrt{\frac{15}{2\pi}}n_z(n_x \pm in_y), \tag{10}$$

$$Y_{20} = \frac{1}{4}\sqrt{\frac{5}{\pi}}(2n_z^2 - n_x^2 - n_y^2),$$

with the unit vector $\boldsymbol{n}$. The spherical harmonic form Y_ψ in Eq. (9) can be rewritten as where A is a 3×3 complex matrix

given by

$$[A]_{11} = \frac{\sqrt{3}}{2}(\psi_2 + \psi_{-2}) - \frac{1}{\sqrt{2}}\psi_0,$$

$$[A]_{12} = [A]_{21} = \frac{\sqrt{3}i}{2}(\psi_2 - \psi_{-2}),$$

$$[A]_{13} = [A]_{31} = -\frac{\sqrt{3}}{2}(\psi_1 - \psi_{-1}),$$

$$[A]_{22} = -\frac{\sqrt{3}}{2}(\psi_2 + \psi_{-2}) - \frac{1}{\sqrt{2}}\psi_0, \tag{11}$$

$$[A]_{23} = [A]_{32} = -\frac{\sqrt{3}i}{2}(\psi_1 + \psi_{-1}),$$

$$[A]_{33} = \sqrt{2}\psi_0.$$

Because A is the traceless and symmetric having the same property with the order parameter A in Eq. (5), we can regard Eq. (11) as a map between the order parameters of neutron $^3P_2$ superfluids and spin-2 spinor condensates. By using Eq. (11), the density ρ, the spin density $\boldsymbol{S}^2$, and the singlet-pair amplitude Ψ_{20} can be rewritten as

$$\rho = \frac{1}{3}(\text{tr}A^*A), \quad \Psi_{20} = \frac{1}{3}(\text{tr}A^2),$$

$$\boldsymbol{S}^2 = \frac{4}{9}(\text{tr}A^*A)^2 + \frac{2}{9}|\text{tr}A^2|^2 - \frac{4}{3}(\text{tr}A^{*2}A^2). \tag{12}$$

The Hamiltonian density h in Eq. (2) for the spinor condensates can be rewritten as

$$h_0 = \frac{\hbar^2}{6m_b}\sum_{i,j,k=x,y,z}\partial_i A_{jk}\partial_i A_{jk}^*,$$

$$h_{qz} = -2q\left[\boldsymbol{B}^T(A^*A)\boldsymbol{B} - \frac{2}{3}(\text{tr}A^*A)\boldsymbol{B}^2\right] \tag{13}$$

$$h_{int} = \frac{c_0 + 4c_1}{18}(\text{tr}A^*A)^2 - \frac{2c_1}{3}(\text{tr}A^{*2}A^2)$$

$$+ \frac{2c_1 + c_2}{18}(\text{tr}A^{*2})(\text{tr}A^2)$$

in terms of the traceless symmetric tensor A. Apart from apparent absence of higher order terms of A, one can observe that the gradient term $f_{202}^{(1)}$ in Eq. (6) for $^3P_2$ superfluids is absent in this case. At the fourth order, the last term in h_{int} is absent in Eq. (6). As for the interaction with the magnetic field $\boldsymbol{B}$, the second term in h_{qz} is absent in Eq. (6) at this order.

B. $^3P_2$ superfluids in terms of five component condensates Ψ

On the other hand, the free-energy density f in Eq. (5) for neutron $^3P_2$ superfluids can be rewritten as

$$f_{202}^{(0)} = 3\boldsymbol{j}^\dagger \cdot \boldsymbol{j},$$

$$f_{202}^{(1)} = 4\boldsymbol{j}^\dagger \cdot \boldsymbol{j} - \frac{i}{2}\boldsymbol{j}^\dagger \cdot \hat{\boldsymbol{S}} \times \boldsymbol{j} - (\boldsymbol{j}^\dagger \cdot \hat{\boldsymbol{S}})(\hat{\boldsymbol{S}} \cdot \boldsymbol{j}),$$

$$f_{002} = 3\rho, \quad f_{004} = 6\rho^2 + \frac{3}{4}\boldsymbol{S}^2 - \frac{3}{2}|\Psi_{20}|^2,$$

$$f_{006} = -324\rho^3 - 81\rho\boldsymbol{S}^2 + 162\rho|\Psi_{20}|^2$$
$$\quad + 15|\Psi_{30}|^2 - 27|\Phi_{30}|^2,$$

$$f_{008} = 6480\rho^4 + 1944\rho^2\boldsymbol{S}^2 - 5184\rho^2|\Psi_{20}|^2$$
$$\quad - 864\rho|\Psi_{30}|^2 + 2592\rho|\Phi_{30}|^2 + 81\boldsymbol{S}^4 \quad\quad (14)$$
$$\quad + 648|\Psi_{20}|^4 - 1296\Gamma_4$$

$$f_{022} = 2\rho\boldsymbol{B}^2 - \frac{1}{2}\psi^\dagger \hat{S}_{\boldsymbol{B}}\hat{S}_{\boldsymbol{B}}\psi,$$

$$f_{024} = \left(-100\rho^2 + 3\boldsymbol{S}^2 + 16|\Psi_{20}|^2\right)\boldsymbol{B}^2$$
$$\quad + \Big[22\rho\psi^\dagger \hat{S}_{\boldsymbol{B}}\hat{S}_{\boldsymbol{B}}\psi + \text{Re}\big(\Psi_{20}^*\psi^T \hat{S}_{\boldsymbol{B}}^T \hat{T}\hat{S}_{\boldsymbol{B}}\psi\big)$$
$$\quad + \frac{5}{4}\Psi_{22}^\dagger \hat{S}_{\boldsymbol{B}}\hat{S}_{\boldsymbol{B}}\Psi_{22} + \frac{1}{2}\Phi_{22}^T \hat{S}_{\boldsymbol{B}}^T \hat{T}\hat{S}_{\boldsymbol{B}}\Phi_{22}\Big],$$

with $\hat{S}_{\boldsymbol{B}} \equiv \hat{\boldsymbol{S}} \cdot \boldsymbol{B}$, where Ψ_{30} and Φ_{30} are SO(3)-invariants, called the singlet trio and the deformed single trio amplitudes, respectively, defined by

$$\Psi_{30} = \frac{\sqrt{2}}{3}\text{tr}(A^3)$$
$$= -\sqrt{\frac{35}{2}} \sum_{J=0}^{4}\sum_{M=-J}^{J}\sum_{m_1,m_2,m_3=-2}^{2}$$
$$\quad \times C_{JM,2m_3}^{00}C_{2m_1,2m_2}^{JM}\psi_{m_1}\psi_{m_2}\psi_{m_3}, \quad\quad (15)$$

$$\Phi_{30} = \frac{\sqrt{2}}{3}\text{tr}(A^*A^2)$$
$$= -\sqrt{\frac{35}{2}} \sum_{J=0}^{4}\sum_{M=-J}^{J}\sum_{m_1,m_2,m_3=-2}^{2}$$
$$\quad \times C_{JM,2m_3}^{00}C_{2m_1,2m_2}^{JM}\psi_{m_1}\psi_{m_2}\varphi_{m_3}^*,$$

respectively, and Γ_4 is an $U(1) \times SO(3)$ invariant, defined by

$$\Gamma_4 = \text{Re}\big[\Psi_{20}\Phi_{30}^{*2}\big] = \frac{2}{27}\text{Re}\{\text{tr}(A^2)[\text{tr}(A^{*2}A)]^2\}. \quad\quad (16)$$

Here Ψ_{22} and Φ_{22} are the quintuplet (spin-2) pair and the deformed quintuplet pair amplitudes, respectively, defined by

$$(\Psi_{22})_M = \sqrt{14}\sum_{m_1,m_2=-2}^{2} C_{2m_1 2m_2}^{2M}\psi_{m_1}\psi_{m_2},$$
$$(17)$$
$$(\Phi_{22})_M = \sqrt{14}\sum_{m_1,m_2=-2}^{2} C_{2m_1 2m_2}^{2M}\psi_{m_1}\varphi_{m_2}^*,$$

where M runs from -2 to 2 for the total spin 2 channel with the Clebsch-Gordan coefficient $C_{2m_1 2m_2}^{2M}$.

IV. CLASSIFYING UNIFORM STATES

In this section, we classify the all possible uniform states with nontrivial unbroken symmetries for f in Eq. (5) and h in Eq. (2), which are called strata in the geometric inviariant theory, as candidates of the ground states or metastable states, and determine the moduli space to which all the uniform states belong.

A. The geometric structure

When $\boldsymbol{B} = 0$, uniform part of the free-energy density $\alpha_0 f_{002} + \beta_0 f_{004} + \gamma_0 f_{006} + \delta_0 f_{008}$ and the Hamiltonian density h_{int} should include only terms which are invariant under the $U(1) \times SO(3)$ transformation $\mathcal{G}_{\text{n,b}}$. Since A or ψ belongs to $\mathbb{C}^5$ and its real dimensions (or degrees of freedom) are 10, there should be $10 - \dim[U(1) \times SO(3)] = 6$ independent $U(1) \times SO(3)$ invariants composed of A or ψ. We can choose them as

$$\left\{\begin{array}{c} \rho, \boldsymbol{S}^2, |\Psi_{20}|^2, \\ |\Psi_{30}|^2, |\Phi_{30}|^2, \Gamma_4 \end{array}\right\} \in \frac{\mathbb{C}^5}{U(1) \times SO(3)} \equiv \mathcal{M}. \quad (18)$$

All of other $U(1) \times SO(3)$ invariants such as $f_{00n \geqslant 10}$ can be written only with these six terms and are not independent. This is a $U(1) \times SO(3)$ orbit space in which subspaces with the same unbroken symmetries are called strata.

In the following, we exclude the case of $\rho = 0$ in which the $U(1) \times SO(3)$ symmetry is fully recovered. Furthermore, we always fix the value of $\rho(> 0)$ because it is irrelevant to the symmetry structure of the uniform states. With fixing ρ and dividing it by $U(1)$ first, we obtain the complex complex projective space $\mathbb{C}P^4$ of the real dimension eight. Dividing it by $SO(3)$, we have a five-dimensional space

$$\left\{\begin{array}{c} \boldsymbol{S}^2, |\Psi_{20}|^2, \\ |\Psi_{30}|^2, |\Phi_{30}|^2, \Gamma_4 \end{array}\right\} \in \frac{\mathbb{C}P^4}{SO(3)} \simeq \mathcal{M}_{\rho=1} \subset \mathcal{M}, \quad (19)$$

parametrized by the five $U(1) \times SO(3)$ invariants instead of Eq. (18). When the uniform state A in f or ψ in h is fixed, the symmetries of the system are further broken from $G_{\text{n,b}}$ down to subgroups $H_{\text{n,b}}$, where $H_{\text{n,b}}$ are the symmetries of the uniform state A and ψ Depending on the nontrivial unbroken symmetries $H_{\text{n,b}}$, there can be nine (15) candidates for the ground (or metastable) states (or strata) with $\boldsymbol{B} = 0$ ($\boldsymbol{B} \neq 0$).

We define $\mathcal{S}$ ($\subset \mathcal{M}_{\rho=1}$) by a space of all uniform states having the nontrivial unbroken symmetry $H_{\text{n,b}}$ under $\boldsymbol{B} = 0$ except for the trivial state $\rho = 0$ where the $U(1) \times SO(3)$ symmetry is fully recovered. In Fig. 1 we show a schematic image of $\mathcal{S}$, consisting of a gray S^2 surface, green, blue, and purple S^1 curves on the S^2 surface, a red S^1 curve connected to the S^2 surface at two points, and a yellow S^1 curve attached to the S^2 and the red curve at points. The dimension for this space is $\dim[\mathcal{S}] = 2$. This is a $U(1) \times SO(3)$ orbit space with nontrivial unbroken symmetries which are not $U(1) \times SO(3)$ or 1. The $U(1) \times SO(3)$ orbits are fibered over $\mathcal{S}$ to recover S^9 of A or ψ with the constraint $\rho = 1$. However, because the total dimension of the space for states
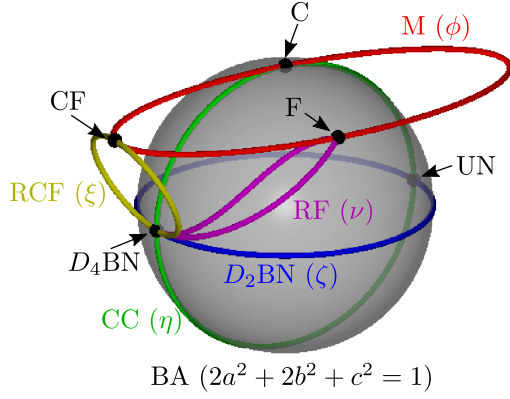
FIG. 1. Schematic image for the topological structure of uniform states having the nontrivial internal symmetries $H_{n,b}$ under $\boldsymbol{B} = 0$.

having the nontrivial symmetries is $\dim\{[U(1) \times SO(3)] \times \mathcal{S}\} = 6$, this space cannot cover S^9 space for A or ψ having nine dimensions. All states having the trivial internal symmetry $H_{n,b} \simeq 1$ constructs the remaining five-dimensional space $(M_{\rho=1} - \mathcal{S})$.

Below we show all of the uniform states having the non-trivial unbroken symmetries $H_{n,b}$ one by one.

B. Ferromagnetic states

The ferromagnetic (F) state ψ_F can be written as

$$\bar{\psi}_F = (1 \quad 0 \quad 0 \quad 0 \quad 0)^T,$$

$$\bar{A}_F = \frac{\sqrt{3}}{2}\begin{pmatrix} 1 & i & 0 \\ i & -1 & 0 \\ 0 & 0 & 0 \end{pmatrix}, \tag{20}$$

where the overbar denotes the normalization as $\bar{\psi} = \psi/\sqrt{\rho}$ and $\bar{A} = A/\sqrt{(\mathrm{tr}A^*A)}$. $\bar{\psi}_F$ and $\bar{A}_F$ are invariant under the transformation $\mathcal{G}^{n,b}(\theta, \hat{z}, \theta/2)$, giving the symmetry $H_{n,b} \simeq U(1) \times \mathbb{Z}_2$ for $\boldsymbol{B} = 0$ or $\boldsymbol{B} \parallel \hat{z}$. Here, θ is the arbitrary real value. For spinor condensates, the F state can be realized for $c_2 > 4c_1$, $c_1 < 0$, and $q = 0$ or $c_2 > 4c_1$, $c_1 < |q|/(2\rho|\boldsymbol{B}|^2)$, and $q < 0$. The F state appears in a certain region of the phase diagram in $^3P_2$ superfluids without the quasiclassical approximation [78].

In terms of invariants, the F state can also be characterized by $\boldsymbol{S}^2 = 4\rho^2$ and $|\Psi_{20}|^2 = |\Psi_{30}|^2 = |\Phi_{30}|^2 = \Gamma_4 = 0$, shown as point F in Fig. 1.

C. Canted ferromagnetic states

The canted ferromagnetic (CF) state ψ_{CF} can be written as

$$\bar{\psi}_{CF} = (0 \quad 1 \quad 0 \quad 0 \quad 0)^T,$$

$$\bar{A}_{CF} = -\frac{\sqrt{3}}{2}\begin{pmatrix} 0 & 0 & 1 \\ 0 & 0 & i \\ 1 & i & 0 \end{pmatrix}. \tag{21}$$

$\bar{\psi}_{CF}$ and $\bar{A}_{CF}$ are invariant under the transformation $\mathcal{G}^{n,b}(\theta, \hat{z}, \theta)$, giving the symmetry $H_{n,b} \simeq U(1)$ for $\boldsymbol{B} = 0$ or $\boldsymbol{B} \parallel \hat{z}$.

In terms of invariants, the CF state can also be characterized by $\boldsymbol{S}^2 = \rho^2$ and $|\Psi_{20}|^2 = |\Psi_{30}|^2 = |\Phi_{30}|^2 = \Gamma_4 = 0$, which is shown as point CF in Fig. 1.

D. Nematic states

The nematic (N) states ψ_N can be written as

$$\bar{\psi}_N = \frac{1}{\sqrt{2}}(\cos\zeta \quad 0 \quad \sqrt{2}\sin\zeta \quad 0 \quad \cos\zeta)^T,$$

$$\bar{A}_N = \sqrt{2}\begin{pmatrix} \cos\lambda_6^+(\zeta) & 0 & 0 \\ 0 & -\cos\lambda_6^-(\zeta) & 0 \\ 0 & 0 & \sin\zeta \end{pmatrix},$$

$$\lambda_n^\pm(x) \equiv x \pm \frac{\pi}{n}, \tag{22}$$

Here ζ is the arbitrary real value. Depending on unbroken symmetries, the nematic states can be further classified into the D_2 biaxial nematic (D_2BN), D_4 biaxial nematic (D_4BN), and uniaxial nematic (UN) states, as explained below. The nematic states are ground-state $^3P_2$ superfluids in the weak coupling limit, within the quasiclassical approximation. The nematic states are shown as the blue S^1 curve in Fig. 1. The extended OPM space $(S^1 \times S^4)/\mathbb{Z}_2$ is fibered over this blue S^1 curve with the fiber $U(1) \times SO(3)/D_2$ [17]. The fiber shrinks at the two points corresponding to the UN and D_4BN states.

1. D_2 biaxial nematic states

For generic ζ, the nematic state is in the D_2BN states, $\bar{\psi}_{D_2BN}$ and $\bar{A}_{D_2BN}$, which are invariant under the transformations $\mathcal{G}^{n,b}(0, \hat{x}, \pi)$ and $\mathcal{G}^{n,b}(0, \hat{z}, \pi)$, giving the symmetry $H_{n,b} \simeq D_2$ and $H_{n,b} \simeq \mathbb{Z}_2$ for $\boldsymbol{B} = 0$ and $\boldsymbol{B} \parallel \hat{z}$, respectively. For spinor condensates, the D_2BN state can be realized for $c_2 < 0$, $c_2 < 4c_1$, and $q = 0$.

In terms of invariants, the D_2BN states can also be characterized by $\boldsymbol{S}^2 = 0$, $|\Psi_{20}|^2 = \rho^2$ and $0 \leqslant |\Psi_{30}|^2/\rho^3 = |\Phi_{30}|^2/\rho^3 = \Gamma_4/\rho^4 \leqslant 1$, which are shown as the blue curve (except for the two points labeled by D_4BN and UN) in Fig. 1.

2. Uniaxial nematic states

One specific case is the uniaxial nematic (UN) state. The UN state ψ_{UN} is the specific state of the nematic state with $\zeta = \pi/2$ in Eq. (22) as

$$\bar{\psi}_{UN} = (0 \quad 0 \quad 1 \quad 0 \quad 0)^T,$$

$$\bar{A}_{UN} = \frac{1}{\sqrt{2}}\begin{pmatrix} -1 & 0 & 0 \\ 0 & -1 & 0 \\ 0 & 0 & 2 \end{pmatrix}. \tag{23}$$

$\bar{\psi}_{UN}$ and $\bar{A}_{UN}$ are invariant under the transformations $\mathcal{G}^{n,b}(0, \hat{x}, \pi)$ and $\mathcal{G}^{n,b}(0, \hat{z}, \theta)$, giving the symmetry $H_{n,b} \simeq D_\infty \simeq O(2)$, $H_{n,b} \simeq U(1)$, and $H_{n,b} \simeq \mathbb{Z}_2$ for $\boldsymbol{B} = 0$, $\boldsymbol{B} \parallel \hat{z}$, and $\boldsymbol{B} \parallel \hat{x}$, respectively. For spinor condensates, the VUN state can be realized for $c_2 \lesssim 4c_1$, $c_2 < 2q/(\rho|\boldsymbol{B}|^2)$, and $q > 0$.

In terms of invariants, the UN state can also be characterized by $\boldsymbol{S}^2 = 0$, $|\Psi_{20}|^2/\rho^2 = |\Psi_{30}|^2/\rho^3 = |\Phi_{30}|^2/\rho^3 = \Gamma_4/\rho^4 = 1$, which is shown as point UN in Fig. 1.

3. D_4 biaxial nematic states

The other specific case is the D_4 biaxial nematic (D_4BN) state, which is also called the square nematic state. The D_4BN state $\psi_{D_4\text{BN}}$ is the specific state of the nematic states with $\zeta = 0$ in Eq. (22) as

$$\bar{\psi}_{D_4\text{BN}} = \frac{1}{\sqrt{2}}(1 \quad 0 \quad 0 \quad 0 \quad 1)^T,$$

$$\bar{A}_{D_4\text{BN}} = \sqrt{\frac{3}{2}}\begin{pmatrix} 1 & 0 & 0 \\ 0 & -1 & 0 \\ 0 & 0 & 0 \end{pmatrix}. \tag{24}$$

$\bar{\psi}_{D_4\text{BN}}$ and $\bar{A}_{D_4\text{BN}}$ are invariant under the transformations $\mathcal{G}^{\text{n,b}}(0, \hat{x}, \pi)$, $\mathcal{G}^{\text{n,b}}(\pi, \hat{z}, \pi/2)$, and $\mathcal{G}^{\text{n,b}}(\pi, (\hat{x}+\hat{y})/\sqrt{2}, \pi)$, giving the symmetry $H_{\text{n,b}} \simeq D_4$, $H_{\text{n,b}} \simeq \mathbb{Z}_4$, $H_{\text{n,b}} \simeq \mathbb{Z}_2$, and $H_{\text{n,b}} \simeq \mathbb{Z}_2$ for $\boldsymbol{B} = 0$, $\boldsymbol{B} \parallel \hat{z}$, $\boldsymbol{B} \parallel \hat{x}$, and $\boldsymbol{B} \parallel (\hat{x}+\hat{y})$, respectively. For spinor condensates, the D_4BN state can be realized for $c_2 < 4c_1$, $c_2 < 2|q|/(\rho|\boldsymbol{B}|^2)$, and $q < 0$.

In terms of invariants, the D_4BN state can also be characterized by $|\Psi_{20}|^2 = \rho^2$ and $\boldsymbol{S}^2 = |\Psi_{30}|^2 = |\Phi_{30}|^2 = \Gamma_4 = 0$, which is shown as point D_4BN in Fig. 1.

E. Cyclic state

The cyclic (C) state ψ_{C} is written as

$$\bar{\psi}_{\text{C}} = \frac{1}{\sqrt{3}}(1 \quad 0 \quad 0 \quad \sqrt{2} \quad 0^T),$$

$$\bar{A}_{\text{C}} = \frac{1}{2}\begin{pmatrix} 1 & i & \sqrt{2} \\ i & -1 & -\sqrt{2}i \\ \sqrt{2} & -\sqrt{2}i & 0 \end{pmatrix}. \tag{25}$$

$\bar{\psi}_{\text{C}}$ and $\bar{A}_{\text{C}}$ are invariant under the transformations $\mathcal{G}^{\text{n,b}}(0, (\sqrt{2}\hat{x}+\hat{z})/\sqrt{3}, \pi)$ and $\mathcal{G}^{\text{n,b}}(-2\pi/3, \hat{z}, 2\pi/3)$, giving the symmetry $H_{\text{n,b}} \simeq T$, $H_{\text{n,b}} \simeq \mathbb{Z}_3$, and $H_{\text{n,b}} \simeq \mathbb{Z}_2$ for $\boldsymbol{B} = 0$, $\boldsymbol{B} \parallel \hat{z}$, and $\boldsymbol{B} \parallel (\sqrt{2}\hat{x}+\hat{z})$, respectively.

The other well-known form of the C state is

$$\mathcal{G}_{\text{C}}^{\text{b}}\bar{\psi}_{\text{C}} = \frac{1}{2}(i \quad 0 \quad \sqrt{2} \quad 0 \quad i)^T,$$

$$\mathcal{G}_{\text{C}}^{\text{n}}\bar{A}_{\text{C}} = \begin{pmatrix} e^{2i\pi/3} & 0 & 0 \\ 0 & e^{-2i\pi/3} & 0 \\ 0 & 0 & 1 \end{pmatrix}, \tag{26}$$

where $\mathcal{G}_{\text{C}}^{\text{n,b}} \equiv \mathcal{G}^{\text{n,b}}(0, \hat{z}, -\pi/4)\mathcal{G}^{\text{n,b}}(0, \hat{y}, -\cos^{-1}(1/\sqrt{3}))$. In this form, $\mathcal{G}_{\text{C}}^{\text{b}}\bar{\psi}_{\text{HC}}$ and $\mathcal{G}_{\text{C}}^{\text{n}}\bar{A}_{\text{HC}}$ are invariant under the transformations $\mathcal{G}^{\text{n,b}}(-2\pi/3, (\hat{x}+\hat{y}+\hat{z})/\sqrt{3}, 2\pi/3)$, and $\mathcal{G}^{\text{n,b}}(0, \hat{z}, \pi)$, giving the symmetry $H_{\text{n,b}} \simeq \mathbb{Z}_2$ and $H_{\text{n,b}} \simeq \mathbb{Z}_3$ for $\boldsymbol{B} \parallel \hat{z}$ and $\boldsymbol{B} \parallel (\hat{x}+\hat{y}+\hat{z})$, respectively. For spinor condensates, the cyclic state can be realized for $c_1 > 0$, $c_2 > 0$, and $q = 0$.

In terms of invariants, the C state can also be characterized by $|\Psi_{30}|^2 = 2\rho^3$ and $\boldsymbol{S}^2 = |\Psi_{20}|^2 = |\Phi_{30}|^2 = \Gamma_4 = 0$, which is shown as point C in Fig. 1.

F. Canted cyclic states

The canted cyclic (CC) states ψ_{CC} are intermediate states interpolating C, UN, and D_4BN states written as

$$\bar{\psi}_{\text{CC}} = \frac{1}{\sqrt{2}}(i\cos\eta \quad 0 \quad \sqrt{2}\sin\eta \quad 0 \quad i\cos\eta)^T,$$

$$\bar{A}_{\text{CC}} = \sqrt{2}\begin{pmatrix} \sigma_\eta & 0 & 0 \\ 0 & \sigma_\eta^* & 0 \\ 0 & 0 & \sin\eta \end{pmatrix},$$

$$\sigma_\eta = \sin\eta\cos(2\pi/3) + i\cos\eta\sin(2\pi/3). \tag{27}$$

The C, UN, and D_4BN states are the specific states with $\eta = \pi/4$, $\pi/2$, and 0, respectively. $\bar{\psi}_{\text{CC}}$ and $\bar{A}_{\text{CC}}$ are invariant under the transformations $\mathcal{G}^{\text{n,b}}(0, \hat{x}, \pi)$ and $\mathcal{G}^{\text{n,b}}(0, \hat{z}, \pi)$, giving the symmetry $H_{\text{n,b}} \simeq D_2$ and $H_{\text{n,b}} \simeq \mathbb{Z}_2$ for $\boldsymbol{B} = 0$ and $\boldsymbol{B} \parallel \hat{z}$. For spinor condensates, the CC state can be realized for $c_2 < 4c_1$, $c_1 > |q|/(2\rho|\boldsymbol{B}|^2)$, $c_2 > 2|q|/(\rho|\boldsymbol{B}|^2)$, and $q \neq 0$.

In terms of the invariants, the CC state can also be characterized by $\boldsymbol{S}^2 = 0$, $0 \leqslant |\Psi_{20}|^2 \leqslant \rho^2$, and

$$|\Psi_{30}|^2 = 2\rho^3 - \frac{3|\Psi_{20}|^4}{2\rho} - \frac{|\Psi_{20}|^6}{2\rho^3},$$

$$|\Phi_{30}|^2 = \frac{|\Psi_{20}|^4}{2\rho} - \frac{|\Psi_{20}|^6}{2\rho^3}, \quad \Gamma_4 = -\frac{|\Psi_{20}|^6}{2\rho^3} + \frac{|\Psi_{20}|^8}{2\rho^5}, \tag{28}$$

which is shown as the green circle in Fig. 1.

G. Reduced ferromagnetic states

The reduced ferromagnetic (RF) states ψ_{RF} are the intermediate states interpolating F and D_4BN states:

$$\bar{\psi}_{\text{RF}} = (\cos\nu \quad 0 \quad 0 \quad 0 \quad \sin\nu)^T,$$

$$\bar{A}_{\text{RF}} = \frac{\sqrt{6}}{2}\begin{pmatrix} \sin\lambda_4^+(\nu) & i\sin\lambda_4^-(\nu) & 0 \\ i\sin\lambda_4^-(\nu) & -\sin\lambda_4^+(\nu) & 0 \\ 0 & 0 & 0 \end{pmatrix}. \tag{29}$$

The F and D_4BN states are the specific states with $\nu = 0$ and $\pi/4$, respectively. $\bar{\psi}_{\text{RF}}$ and $\bar{A}_{\text{RF}}$ are invariant under the transformation $\mathcal{G}^{\text{n,b}}(\pi, \hat{z}, \pi/2)$, giving the symmetry $H_{\text{n,b}} \simeq \mathbb{Z}_4$ for $\boldsymbol{B} = 0$ or $\boldsymbol{B} \parallel \hat{z}$.

In terms of the invariants, the RF states can also be characterized by $0 \leqslant \boldsymbol{S}^2 = 4(\rho^2 - |\Psi_{20}|^2) \leqslant 4\rho^2$, $|\Psi_{30}|^2 = |\Phi_{30}|^2 = \Gamma_4 = 0$, which are shown as the green curve in Fig. 1.

H. Reduced canted ferromagnetic state

The reduced canted ferromagnetic (RCF) states ψ_{RCF} are intermediate states interpolating the CF and D_4BN states:

$$\bar{\psi}_{\text{RCF}} = (0 \quad \cos\xi \quad 0 \quad \sin\xi \quad 0)^T,$$

$$\bar{A}_{\text{RCF}} = -\frac{\sqrt{6}}{2}\begin{pmatrix} 0 & 0 & \sin\lambda_4^-(\xi) \\ 0 & 0 & i\sin\lambda_4^+(\xi) \\ \sin\lambda_4^-(\xi) & i\sin\lambda_4^+(\xi) & 0 \end{pmatrix}. \tag{30}$$

The F and D_4BN states are the specific states with $\xi = 0$ and $\pi/4$, respectively. $\bar{\psi}_{\text{RCF}}$ and $\bar{A}_{\text{RCF}}$ are invariant under the transformation $\mathcal{G}^{\text{n,b}}(\pi, \hat{z}, \pi)$, giving the symmetry $H_{\text{n,b}} \simeq \mathbb{Z}_2$ for $\boldsymbol{B} = 0$ or $\boldsymbol{B} \parallel \hat{z}$.

In terms of the invariants, the RF states can also be characterized by $0 \leqslant S^2 = \rho^2 - |\Psi_{20}|^2 \leqslant \rho^2$, $|\Psi_{30}|^2 = |\Phi_{30}|^2 = \Gamma_4 = 0$, shown as the green curve in Fig. 1.

I. Mixed state

The mixed (M) states ψ_M are intermediate states interpolating the C, F, and CF states, which can be written as

$$\bar{\psi}_M = (\cos\phi \quad 0 \quad 0 \quad \sin\phi \quad 0)^T,$$

$$\bar{A}_M = \frac{\sqrt{3}}{2}\begin{pmatrix} \cos\phi & i\cos\phi & \sin\phi \\ i\cos\phi & -\cos\phi & -i\sin\phi \\ \sin\phi & -i\sin\phi & 0 \end{pmatrix}. \quad (31)$$

The C, F, and CF states are the specific states with $\phi = \cos^{-1}(1/\sqrt{3})$, $\phi = 0$, and $\phi = \pi/2$, respectively. $\bar{\psi}_M$ and $\bar{A}_M$ are invariant under the transformation $\mathcal{G}^{n,b}(-2\pi/3, \hat{z}, 2\pi/3)$, giving the symmetry $H_{n,b} \simeq \mathbb{Z}_3$ for $\boldsymbol{B} = 0$ or $\boldsymbol{B} \parallel \hat{z}$. For spinor condensates, the M state can be realized for $c_2 > 4c_1$, $c_1 > |q|/(2\rho|\boldsymbol{B}|^2)$, $c_2 > 2|q|/(\rho|\boldsymbol{B}|^2)$, and $q < 0$.

In terms of the invariants, the M states can also be characterized by $-\rho^2 \leqslant (S^2)^{1/2} \leqslant 4\rho^2$, $|\Psi_{20}|^2 = |\Phi_{30}|^2 = 0$, and

$$|\Psi_{30}|^2 = \frac{4\rho^3 - 3\rho S^2 + (S^2)^{3/2}}{2}, \quad (32)$$

which are shown as the green curve in Fig. 1.

J. Broken axisymmetric states

The broken axisymmetric (BA) states are intermediate states interpolating the RF and CC states, which can be written as

$$\bar{\psi}_{BA} = (a+b \quad 0 \quad c \quad 0 \quad a-b)^T,$$

$$\bar{A}_{BA} = \frac{1}{\sqrt{2}}\begin{pmatrix} \sqrt{6}a - c & \sqrt{6}ib & 0 \\ \sqrt{6}ib & -\sqrt{6}a - c & 0 \\ 0 & 0 & 2c \end{pmatrix}. \quad (33)$$

Here a, b, and c are arbitrary real values satisfying $1 = 2(a^2 + b^2) + c^2$. RF and CC states are the specific states with $c = 0$ and $a = 0$, respectively. $\bar{\psi}_{BA}$ and $\bar{A}_{BA}$ are invariant under the transformation or $\mathcal{G}^{n,b}(0, \hat{z}, \pi)$, giving the symmetry $H_{n,b} \simeq \mathbb{Z}_2$ for $\boldsymbol{B} = 0$ or $\boldsymbol{B} \parallel \hat{z}$. For spinor condensates, the BA state can be realized for $c_2 \gtrsim 4c_1$, $q > 0$, and $\boldsymbol{B} \parallel \hat{x}$ where the symmetry becomes trivial $H_{n,b} \simeq 1$. The BA states (also called magnetized BN states in Ref. [78]) appear in a certain region of the phase diagram for $\boldsymbol{B} \parallel \hat{z}$ in $^3P_2$ superfluids without the quasiclassical approximation [78].

In terms of the invariants, the BA states can also be characterized by $0 \leqslant S^2 \leqslant 4\rho^2$, $-(\rho^2 - S^2/4) \leqslant (|\Psi_{20}|^2)^{1/2} \leqslant \rho^2 - S^2/4$, and

$$|\Psi_{30}|^2 = \frac{\chi\rho^2\{4\rho^2 - S^2 + 6(|\Psi_{20}|^2)^{1/2}\rho + 2|\Psi_{20}|^2\}^2}{32\{\rho + (|\Psi_{20}|^2)^{1/2}\}^3},$$

$$|\Phi_{30}|^2 = \frac{\chi\rho^2\{S^2 + 2(|\Psi_{20}|^2)^{1/2}\rho + 2|\Psi_{20}|^2\}^2}{32\{\rho + (|\Psi_{20}|^2)^{1/2}\}^3},$$
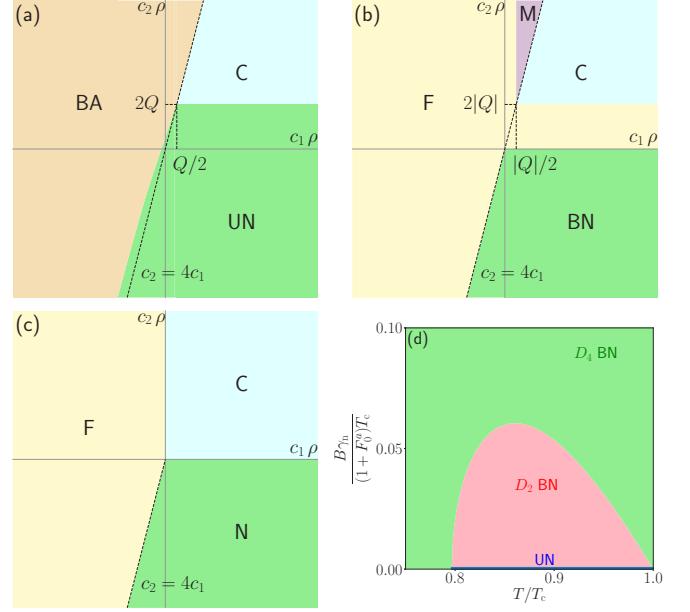

FIG. 2. Phase diagram for the spinor condensates (a)–(c) and the neutron $^3P_2$ superfluid (d). In panels (a), (b), and (c), the coefficient of the quadratic Zeeman energy $Q \equiv q|\boldsymbol{B}|^2$ is positive, negative, and zero, respectively. In panel (a), the boundary between the BA and UN states can be numerically determined. In panel (d), the UN ($B = 0$) and D_2BN ($B > 0$) states appear only at $T \gtrsim 0.796$. The critical magnetic field between D_2BN and D_4BN states takes the maximal $B = 6.05 \times 10^{-3}(1 + F_0^a)T_c/\gamma_n$ at $T = 0.860T_c$.

$$\Gamma_4 = (|\Psi_{20}|^2)^{1/2}|\Phi_{30}|^2,$$

$$\chi \equiv 4 - \frac{S^2}{\rho^2} - \frac{4|\Psi_{20}|^2}{\rho^2}, \quad (34)$$

which are shown as the gray surface in Fig. 1.

K. Phase diagram and topological structure for symmetric uniform state

In Fig. 2 we show phase diagrams for the spinor condensates for the Hamiltonian density h in Eq. (1) and neutron superfluid for the free-energy density f in Eq. (5). For spinor condensates, the F, M, C, and BN (BA, C, and UN) states appear for $q > 0$ ($q < 0$). In the case of $q = 0$, the F, C, and N states appear, and all states (D_2BN, D_4BN, and UN states) in the N states are degenerated.

For neutron $^3P_2$ superfluids, the UN, D_2BN, and D_4BN states are dominant within the present framework, which corresponds to the region with positive c_1 and negative c_2 for the spinor condensates. At high temperatures, the D_4BN and D_2BN (UN) states appear for $\boldsymbol{B} \neq 0$ ($\boldsymbol{B} = 0$). At low temperatures, the only D_4BN state appears, which contradicts the result obtained by the BdG analysis [74] giving the D_4BN, D_2BN, and UN states at any temperature. This contradiction originates from the fact that the GL expansion is valid only around the critical temperature, and this discrepancy may be cured by including higher order terms into the free-energy density f in Eq. (5), which neglects terms higher than the eighth order. Besides these three states, the existences of the

TABLE I. $U(1) \times SO(3)$ invariant terms $\boldsymbol{S}^2$, $|\Psi_{20}|^2$, $|\Psi_{30}|^2$, $|\Phi_{30}|^2$, and Γ_4, and unbroken symmetry $H_{n,b}$ for uniform ground states. Here $F(x)$ defined as the expansion with $\cos(2x)$: $F^{(n)}_{a_0,\cdots a_n}(x) \equiv \sum_{k=0}^{n} a_k \cos^k(2x)$ and $F^{\pm}_{ab} \equiv (1 - 8a^2 \pm 4b^2)^2$.

State	$\boldsymbol{S}^2/\rho^2$	$|\Psi_{20}|^2/\rho^2$	$|\Psi_{30}|^2/\rho^3$	$|\Phi_{30}|^2/\rho^3$	Γ_4/ρ^4	$H_{n,b}$
F	4	0	0	0	0	$[U(1) \times \mathbb{Z}_2]_{\boldsymbol{B}=0,\,\boldsymbol{B}\parallel\hat{z}}$
CF	1	0	0	0	0	$[U(1)]_{\boldsymbol{B}=0,\,\boldsymbol{B}\parallel\hat{z}}$
D_2BN	0	1	$\sin^2(3\zeta)$	$\sin^2(3\zeta)$	$\sin^2(3\zeta)$	$[D_2]_{\boldsymbol{B}=0},\,[\mathbb{Z}_2]_{\boldsymbol{B}\parallel\hat{z}}$
UN	0	1	1	1	1	$[D_\infty]_{\boldsymbol{B}=0},\,[U(1)]_{\boldsymbol{B}\parallel\hat{z}},\,[\mathbb{Z}_2]_{\boldsymbol{B}\parallel\hat{x}}$
D_4BN	0	1	0	0	0	$[D_4]_{\boldsymbol{B}=0},\,[\mathbb{Z}_4]_{\boldsymbol{B}\parallel\hat{z}},\,[\mathbb{Z}_2]_{\boldsymbol{B}\parallel\hat{x},\,\boldsymbol{B}\parallel(\hat{x}+\hat{y})}$
C	0	0	2	0	0	$[T]_{\boldsymbol{B}=0},\,[\mathbb{Z}_3]_{\boldsymbol{B}\parallel\hat{z}},\,[\mathbb{Z}_2]_{\boldsymbol{B}\parallel(\sqrt{2}\hat{x}+\hat{z})}$
CC	0	$\cos^2(2\eta)$	$\frac{1}{2}F^{(3)}_{4,0,-3,-1}(\eta)$	$\frac{1}{2}F^{(3)}_{0,0,1,-1}(\eta)$	$\frac{1}{2}F^{(4)}_{0,0,0,-1,1}(\eta)$	$[D_2]_{\boldsymbol{B}=0},\,[\mathbb{Z}_2]_{\boldsymbol{B}\parallel\hat{z}}$
RF	$4\cos^2(2\nu)$	$\sin^2(2\nu)$	0	0	0	$[\mathbb{Z}_4]_{\boldsymbol{B}=0,\,\boldsymbol{B}\parallel\hat{z}}$
RCF	$\cos^2(2\xi)$	$\sin^2(2\xi)$	0	0	0	$[\mathbb{Z}_2]_{\boldsymbol{B}=0,\,\boldsymbol{B}\parallel\hat{z}}$
M	$\frac{1}{4}F^{(2)}_{1,6,9}(\phi)$	0	$\frac{27}{16}F^{(3)}_{1,-1,-1,1}(\phi)$	0	0	$[\mathbb{Z}_3]_{\boldsymbol{B}=0,\,\boldsymbol{B}\parallel\hat{z}}$
BA	$64a^2b^2$	$(1-4b^2)^2$	$F^+_{ab}c^2$	$F^-_{ab}c^2$	$(1-4b^2)F^-_{ab}c^2$	$[\mathbb{Z}_2]_{\boldsymbol{B}=0,\,\boldsymbol{B}\parallel\hat{z}}$

F and BA states [4] are also predicted [78] without the quasi-classical approximation that we use to obtain the free-energy density f in Eq. (5) from the Lagrangian $\mathcal{L}$ in Eq. (4)

Now let us go back to Fig. 1 in which we have shown all the states having the nontrivial symmetry $H_{n,b}$ under $\boldsymbol{B} = 0$ explained above. The BA states for $2a^2 + 2b^2 + c^2 = 1$ are represented by the gray S^2 surface, and the D_2BN, CC, RF states are denoted by the green, blue, and purple S^1 curves parametrized by ζ, η, and ν, respectively. The S^2 surface can also be constructed with the $U(1) \times SO(3)$-invariants $\{\boldsymbol{S}^2, |\Psi_{20}|^2, |\Psi_{30}|^2, |\Phi_{30}|^2, \Gamma_4\}$ under the constraints shown in Eq. (34). The RCF state is represented by the S^1 curves for ξ out of the S^2 surface for the BN state except for the point corresponding to D_4BN states. The M state is represented by the S^1 curves for ϕ out of the S^2 surface for the BN state except for two points corresponding to C and F states. The F, UN, and D_4BN states correspond to the points on the S^2 surface for the BN state, while the CF state corresponds to the point out of the S^2 surface for the BN state.

V. $^3P_2$ NEUTRON SUPERFLUIDS

When $\boldsymbol{B} = 0$, uniform part of the free-energy density $\alpha f_{002} + \beta_0 f_{004} + \gamma_0 f_{006} + \delta_0 f_{008}$ and the Hamiltonian density h_{int} includes only terms which are invariant under the $U(1) \times SO(3)$ transformation $\mathcal{G}_{n,b}$. Because the internal degrees of freedom for A or ψ are nine after fixing ρ, there are five independent $U(1) \times SO(3)$ invariant terms. We fix them as $\boldsymbol{S}^2$, $|\Psi_{20}|^2$, $|\Psi_{30}|^2$, $|\Phi_{30}|^2$, and Γ_4. In Table I we summarize them and unbroken symmetries in the free-energy density f for each uniform ground state. In Table II we also summarize components $\boldsymbol{S}^2$, $|\Psi_{20}|^2$, $|\Psi_{30}|^2$, and $|\Phi_{30}|^2$ and components in the free-energy density f for each uniform ground state, respectively. For the BA state, some results are too long to be shown in the table, and we write them here:

$$\frac{f_{004}}{\rho^2} = \frac{9}{2} + 12(1 + 4a^2 - 2b^2)b^2, \tag{35}$$

$$\frac{f_{006}}{\rho^3} = -6[29 - 4a^2(3 - 8a^2)^2 + 156b^2 \\ + 48a^2(31 - 24a^2)b^2 - 96(3 + 10a^2)b^4 - 64b^6], \tag{36}$$

$$\frac{f_{008}}{\rho^4} = 216[11 - 4a^2(3 - 8a^2)^2 + 84b^2 \\ + 48a^2(21 + 16a^2 - 64a^4)b^2 \\ - 48(3 - 28a^2 + 96a^4)b^4 - 64(1 + 60a^2)b^6]. \tag{37}$$

We further show

$$\frac{f_{022}}{\rho B^2} = 2c^2, \tag{38}$$

$$\frac{f_{024}}{\rho^2 B^2} = -12(6a^2 + 10b^2 + 7c^2)c^2, \tag{39}$$

for $\boldsymbol{B} \parallel \hat{z}$, and

$$\frac{f_{022}}{\rho B^2} = \frac{3}{2} - (\sqrt{6}a + c)c, \tag{40}$$

$$\frac{f_{024}}{\rho^2 B^2} = -6[2 + 22a^2 + 18b^2 - 8(a^2 - b^2)(2a^2 - b^2) \\ - \sqrt{6}ac(8a^2 - 4b^2 + 5)], \tag{41}$$

for $\boldsymbol{B} \parallel \hat{x}$.

In Table II we also highlight the lowest values for each terms. At the temperature close to the superfluid transition temperature T_c, the N state (D_2BN, UN, and D_4BN states) has the lowest value of $f_{004} = (9/2)\rho^2$, and the UN (D_4BN) state has the lower value of $f_{006} = -174\rho^3$ ($f_{008} = 1944\rho^4$) than other nematic states. Under the magnetic field, the D_4BN (UN) state with $\boldsymbol{B} \parallel \hat{z}$ has a lower value of $f_{022} = 0$ ($f_{024} = -84\rho^2 B^2$) than other nematic states. Actually, UN, D_4BN, and D_2BN states are predicted to be realized within the GL expansion in Eq. (5) [54].

VI. SUMMARY AND DISCUSSION

In this paper, we have discussed a relationship between the neutron $^3P_2$ superfluids and spin-2 spinor BECs, the formalism of which is usually written with the 3×3 traceless symmetric tensor A and the five-component condensate wave functions ψ, respectively. Because A and ψ have the same internal

TABLE II. Components of free-energy density f for uniform ground states. The lowest values for each term are highlighted with underlining.

State	f_{004}/ρ^2	f_{006}/ρ^3	f_{008}/ρ^4	$f_{022}/(\rho B^2)$	$f_{024}/(\rho^2 B^2)$
$[\text{F}]_{\boldsymbol{B}\parallel\hat{z}}$	9	$\underline{-648}$	15 552	$\underline{0}$	0
$[\text{CF}]_{\boldsymbol{B}\parallel\hat{z}}$	$\frac{27}{4}$	-405	8505	$\frac{3}{2}$	-45
$[\text{UN}]_{\boldsymbol{B}\parallel\hat{z}}$	$\frac{9}{2}$	-174	2376	2	$\underline{-84}$
$[D_4\text{BN}]_{\boldsymbol{B}\parallel\hat{z}}$	$\frac{9}{2}$	-162	$\underline{1944}$	$\underline{0}$	0
$[D_4\text{BN}]_{\boldsymbol{B}\parallel\hat{x},\,\boldsymbol{B}\parallel(\hat{x}+\hat{y})}$	$\frac{9}{2}$	-162	$\underline{1944}$	$3/2$	-54
$[D_2\text{BN}]_{\boldsymbol{B}\parallel\hat{z}}$	$\frac{9}{2}$	$-6F^{(3)}_{28,3,0,-4}(\zeta)$	$216F^{(3)}_{10,3,0,-4}(\zeta)$	$F^{(1)}_{1,-1}(\zeta)$	$-6F^{(2)}_{5,-7,2}(\zeta)$
$[\text{C}]_{\boldsymbol{B}\parallel\hat{z},\,\boldsymbol{B}\parallel(\sqrt{2}\hat{x}+\hat{z})}$	6	-294	4752	1	-36
$[\text{CC}]_{\boldsymbol{B}\parallel\hat{z}}$	$\frac{3}{2}F^{(2)}_{4,0,-1}(\eta)$	$-6F^{(3)}_{49,0,-21,-1}(\eta)$	$216F^{(3)}_{22,0,-12,-1}(\eta)$	$F^{(1)}_{1,-1}(\eta)$	$-6F^{(2)}_{6,-7,1}(\eta)$
$[\text{RF}]_{\boldsymbol{B}\parallel\hat{z}}$	$\frac{9}{2}F^{(2)}_{1,0,1}(\nu)$	$-162F^{(2)}_{1,0,3}(\nu)$	$1944F^{(4)}_{1,0,6,0,1}(\nu)$	0	0
$[\text{RCF}]_{\boldsymbol{B}\parallel\hat{z}}$	$\frac{9}{4}F^{(2)}_{2,0,1}(\xi)$	$-81F^{(2)}_{2,0,3}(\xi)$	$243F^{(4)}_{8,0,24,0,3}(\xi)$	$3/2$	$-9F^{(2)}_{5,0,-1}(\xi)$
$[\text{M}]_{\boldsymbol{B}\parallel\hat{z}}$	$\frac{9}{16}F^{(2)}_{11,2,3}(\phi)$	$-\frac{81}{16}F^{(3)}_{63,29,41,-5}(\phi)$	$\frac{243}{16}F^{(4)}_{363,292,402,-60,27}(\phi)$	$\frac{3}{4}F^{(1)}_{1,-1}(\phi)$	$-\frac{9}{4}F^{(2)}_{13,-10,-3}(\phi)$
$[\text{BA}]_{\boldsymbol{B}\parallel\hat{z}}$	Eq. (35)	Eq. (36)	Eq. (37)	Eq. (38)	Eq. (39)
$[\text{BA}]_{\boldsymbol{B}\parallel\hat{x}}$	Eq. (35)	Eq. (36)	Eq. (37)	Eq. (40)	Eq. (41)

degrees of freedom, they are transformed to each other, and we have shown the correspondence between the free-energy density f for the neutron superfluids and the low-energy density h for spin-2 spinor BECs in the both languages of A and ψ. We also have listed 15 uniform states having the internal symmetry as the candidate of the possible ground states for neutron $^3P_2$ superfluids.

In this paper, we have started from the low-energy functional h in Eq. (1) and the GL free-energy density f in Eq. (5), which are effective theory restricted at $T = 0$ and $T \approx T_c$, respectively. We need to use a different framework beyond these temperature regions. For example, we have to use the BdG theory [74] for neutron $^3P_2$ superfluidity near $T = 0$ (see Ref. [34] for $^3P_2$-$^3F_2$ pairing). Once we find new candidates for stable states, our results will immediately give information for such new states via Table I.

We hope that our present work will lead a deeper understanding of neutron $^3P_2$ superfluids, spin-2 spinor BECs, their relationship, and a systematic way to discuss possible ground states. Although not all states appear as the ground states or metastable states in either spin-2 spinor BEC or $^3P_2$ superfluids, some may appear, for instance, as metastable states at spin-2 spinor BECs with higher order interaction

terms such as three- and four-body scattering, or higher order expansions of the GL theory for the $^3P_2$ superfluids. Another application of our present work is local structures in a vortex core at which the different symmetric state may appear from that surrounding the vortex in the bulk. We can discuss which state is filled at the vortex core by calculating S^2, $|\Psi_{20}|^2$, $|\Psi_{30}|^2$, $|\Phi_{30}|^2$, and so on. We will report on this topic elsewhere.

In Ref. [55] a mixture of a $^3P_2$ neturon superfluid and a $^1S_0$ neutron superfluid, which may be realized in the intermediate region of neutron star cores, was discussed. This situation corresponds to a mixture of a spin-2 spinor BEC and a scalar BEC.

[1] D. Vollhardt and P. Wölfle, *The Superfluid Phases of Helium 3*, Dover Books on Physics Series (Dover Publications, New York, 2013).

[2] G. E. Volovik, *The Universe in a Helium Droplet* (Clarendon, Oxford, 2003).

[3] N. D. Mermin, Phys. Rev. A **9**, 868 (1974).

[4] Y. Kawaguchi and M. Ueda, Phys. Rep. **520**, 253 (2012).

[5] H. Schmaljohann, M. Erhard, J. Kronjäger, M. Kottke, S. van Staa, L. Cacciapuoti, J. J. Arlt, K. Bongs, and K. Sengstock, Phys. Rev. Lett. **92**, 040402 (2004).

[6] M.-S. Chang, C. D. Hamley, M. D. Barrett, J. A. Sauer, K. M. Fortier, W. Zhang, L. You, and M. S. Chapman, Phys. Rev. Lett. **92**, 140403 (2004).

[7] T. Kuwamoto, K. Araki, T. Eno, and T. Hirano, Phys. Rev. A **69**, 063604 (2004).

[8] A. Widera, F. Gerbier, S. Fölling, T. Gericke, O. Mandel, and I. Bloch, New J. Phys. **8**, 152 (2006).

[9] S. Tojo, A. Tomiyama, M. Iwata, T. Kuwamoto, and T. Hirano, Appl. Phys. B **93**, 403 (2008).

[10] S. Tojo, T. Hayashi, T. Tanabe, T. Hirano, Y. Kawaguchi, H. Saito, and M. Ueda, Phys. Rev. A **80**, 042704 (2009).

[11] The cyclic phase is also discussed in a superconductor [87].

[12] S. Kobayashi, M. Kobayashi, Y. Kawaguchi, M. Nitta, and M. Ueda, Nucl. Phys. B **856**, 577 (2012).

[13] G. W. Semenoff and F. Zhou, Phys. Rev. Lett. **98**, 100401 (2007).

[14] M. Kobayashi, Y. Kawaguchi, M. Nitta, and M. Ueda, Phys. Rev. Lett. **103**, 115301 (2009).

[15] T. Mawson, T. C. Petersen, J. K. Slingerland, and T. P. Simula, Phys. Rev. Lett. **123**, 140404 (2019).

[16] K. Tiurev, T. Ollikainen, P. Kuopanportti, M. Nakahara, D. S. Hall, and M. Möttönen, New J. Phys. **20**, 055011 (2018).

[17] S. Uchino, M. Kobayashi, and M. Ueda, Phys. Rev. A **81**, 063632 (2010).

[18] S. Uchino, M. Kobayashi, M. Nitta, and M. Ueda, Phys. Rev. Lett. **105**, 230406 (2010).

[19] M. O. Borgh and J. Ruostekoski, Phys. Rev. Lett. **117**, 275302 (2016); **118**, 129901(E) (2017).

[20] F. Tabakin, Phys. Rev. **174**, 1208 (1968).

[21] M. Hoffberg, A. E. Glassgold, R. W. Richardson, and M. Ruderman, Phys. Rev. Lett. **24**, 775 (1970).

[22] R. Tamagaki, Prog. Theor. Phys. **44**, 905 (1970).

[23] T. Takatsuka and R. Tamagaki, Prog. Theor. Phys. **46**, 114 (1971).

[24] T. Takatsuka, Prog. Theor. Phys. **47**, 1062 (1972).

[25] T. Fujita and T. Tsuneto, Prog. Theor. Phys. **48**, 766 (1972).

[26] R. W. Richardson, Phys. Rev. D **5**, 1883 (1972).

[27] L. Amundsen and E. Ostgaard, Nucl. Phys. A **442**, 163 (1985).

[28] T. Takatsuka and R. Tamagaki, Prog. Theor. Phys. Suppl. **112**, 27 (1993).

[29] M. Baldo, J. Cugnon, A. Lejeune, and U. Lombardo, Nucl. Phys. A **536**, 349 (1992).

[30] O. Elgaroy, L. Engvik, M. Hjorth-Jensen, and E. Osnes, Nucl. Phys. A **607**, 425 (1996).

[31] V. A. Khodel, V. V. Khodel, and J. W. Clark, Phys. Rev. Lett. **81**, 3828 (1998).

[32] M. Baldo, O. Elgaroy, L. Engvik, M. Hjorth-Jensen, and H. J. Schulze, Phys. Rev. C **58**, 1921 (1998).

[33] V. V. Khodel, V. A. Khodel, and J. W. Clark, Nucl. Phys. A **679**, 827 (2001).

[34] M. V. Zverev, J. W. Clark, and V. A. Khodel, Nucl. Phys. A **720**, 20 (2003).

[35] N. Chamel and P. Haensel, Living Rev. Rel. **11**, 10 (2008).

[36] S. Maurizio, J. W. Holt, and P. Finelli, Phys. Rev. C **90**, 044003 (2014).

[37] S. K. Bogner, R. J. Furnstahl, and A. Schwenk, Prog. Part. Nucl. Phys. **65**, 94 (2010).

[38] S. Srinivas and S. Ramanan, Phys. Rev. C **94**, 064303 (2016).

[39] B. Haskell and A. Sedrakian, Astrophys. Space Sci. Libr. **457**, 401 (2018).

[40] N. Chamel, J. Astrophys. Astron. **38**, 43 (2017).

[41] A. Sedrakian and J. W. Clark, Eur. Phys. J. A **55**, 167 (2019).

[42] V. Graber, N. Andersson, and M. Hogg, Int. J. Mod. Phys. D **26**, 1730015 (2017).

[43] N. Andersson, Universe **7**, 17 (2021).

[44] C. O. Heinke and W. C. G. Ho, Astrophys. J. **719**, L167 (2010).

[45] P. S. Shternin, D. G. Yakovlev, C. O. Heinke, W. C. G. Ho, and D. J. Patnaude, Mon. Not. R. Astron. Soc. Lett. **412**, L108 (2011).

[46] D. Page, M. Prakash, J. M. Lattimer, and A. W. Steiner, Phys. Rev. Lett. **106**, 081101 (2011).

[47] J. A. Sauls and J. W. Serene, Phys. Rev. D **17**, 1524 (1978).

[48] P. Muzikar, J. A. Sauls, and J. W. Serene, Phys. Rev. D **21**, 1494 (1980).

[49] J. A. Sauls, D. L. Stein, and J. W. Serene, Phys. Rev. D **25**, 967 (1982).

[50] V. Z. Vulovic and J. A. Sauls, Phys. Rev. D **29**, 2705 (1984).

[51] K. Masuda and M. Nitta, Phys. Rev. C **93**, 035804 (2016).

[52] S. Yasui, C. Chatterjee, and M. Nitta, Phys. Rev. C **99**, 035213 (2019).

[53] S. Yasui, C. Chatterjee, and M. Nitta, *Proceedings of the Eighth International Conference on Quarks and Nuclear Physics (QNP2018): Tsukuba, Japan, November 13–17, 2018*, JPS Conf. Proc. **26**, 024022 (2019).

[54] S. Yasui, C. Chatterjee, M. Kobayashi, and M. Nitta, Phys. Rev. C **100**, 025204 (2019).

[55] S. Yasui, D. Inotani, and M. Nitta, Phys. Rev. C **101**, 055806 (2020).

[56] P. F. Bedaque, G. Rupak, and M. J. Savage, Phys. Rev. C **68**, 065802 (2003).

[57] L. B. Leinson, Phys. Lett. B **702**, 422 (2011).

[58] L. B. Leinson, Phys. Rev. C **85**, 065502 (2012).

[59] L. B. Leinson, Phys. Rev. C **87**, 025501 (2013).

[60] P. F. Bedaque and A. N. Nicholson, Phys. Rev. C **87**, 055807 (2013); **89**, 029902(E) (2014).

[61] P. Bedaque and S. Sen, Phys. Rev. C **89**, 035808 (2014).

[62] P. F. Bedaque and S. Reddy, Phys. Lett. B **735**, 340 (2014).

[63] P. F. Bedaque, A. N. Nicholson, and S. Sen, Phys. Rev. C **92**, 035809 (2015).

[64] L. B. Leinson, Phys. Rev. C **81**, 025501 (2010).

[65] L. B. Leinson, Phys. Lett. B **689**, 60 (2010).

[66] L. B. Leinson, Phys. Rev. C **82**, 065503 (2010); **84**, 049901(E) (2011).

[67] L. B. Leinson, Phys. Rev. C **83**, 055803 (2011).

[68] L. B. Leinson, Phys. Rev. C **84**, 045501 (2011).

[69] C. Chatterjee, M. Haberichter, and M. Nitta, Phys. Rev. C **96**, 055807 (2017).

[70] K. Masuda and M. Nitta, Prog. Theor. Exp. Phys. **2020**, 013 (2020).

[71] L. B. Leinson, Mon. Not. R. Astron. Soc. **498**, 304 (2020).

[72] S. Yasui and M. Nitta, Phys. Rev. C **101**, 015207 (2020).

[73] S. Yasui, C. Chatterjee, and M. Nitta, Phys. Rev. C **101**, 025204 (2020).

[74] T. Mizushima, K. Masuda, and M. Nitta, Phys. Rev. B **95**, 140503(R) (2017).

[75] T. Mizushima, S. Yasui, and M. Nitta, Phys. Rev. Research **2**, 013194 (2020).

[76] Y. Masaki, T. Mizushima, and M. Nitta, Phys. Rev. Research **2**, 013193 (2020).

[77] Y. Masaki, T. Mizushima, and M. Nitta arXiv:2107.02448.

[78] T. Mizushima, S. Yasui, D. Inotani, and M. Nitta, Phys. Rev. C **104**, 045803 (2021).

[79] M. Abud and G. Sartori, Phys. Lett. B **104**, 147 (1981).

[80] M. Abud and G. Sartori, Ann. Phys. **150**, 307 (1983).

[81] M. Nitta, Int. J. Mod. Phys. A **14**, 2397 (1999).

[82] R. Barnett, A. Turner, and E. Demler, Phys. Rev. Lett. **97**, 180412 (2006).

[83] Y. Kawaguchi and M. Ueda, Phys. Rev. A **84**, 053616 (2011).

[84] B. Lian, T.-L. Ho, and H. Zhai, Phys. Rev. A **85**, 051606(R) (2012).

[85] D. M. Stamper-Kurn and M. Ueda, Rev. Mod. Phys. **85**, 1191 (2013).

[86] D. A. Takahashi, J. Phys. Soc. Jpn. **84**, 025001 (2015).

[87] T. Mizushima and M. Nitta, Phys. Rev. B **97**, 024506 (2018).